

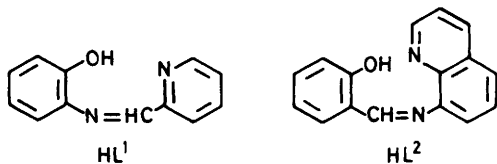
New Spin-crossover Iron(III) Complexes with Large Hysteresis Effects and Time Dependence of their Magnetism †

Hiroki Oshio, Kenji Kitazaki, Junichi Mishiro, Noriyuki Kato, Yonezo Maeda,* and Yoshimasa Takashima

Department of Chemistry, Faculty of Science, Kyushu University, Hakozaki, Higashiku, Fukuoka 812, Japan

The new complexes $[\text{FeL}^1_2]\text{ClO}_4$ ($\text{HL}^1 =$ tridentate Schiff base formed by 1 : 1 condensation of *o*-aminophenol and pyridine-2-carbaldehyde) and $[\text{FeL}^2_2]\text{NCS}$ ($\text{HL}^2 =$ tridentate Schiff base formed by 1 : 1 condensation of 8-aminoquinoline and salicylaldehyde) were synthesized. The spin-crossover behaviour between $S = \frac{1}{2}$ and $\frac{5}{2}$ which is dependent on temperature was observed for the solid complexes using variable-temperature ^{57}Fe Mössbauer spectral and magnetic measurements. Both compounds show a pronounced hysteresis effect in the high spin \rightleftharpoons low spin transition. For $[\text{FeL}^1_2]\text{ClO}_4$, sharp and strong Mössbauer absorptions were observed over the temperature range examined and the effective vibrating mass, M_{eff} , was evaluated using the high-temperature approximation of the Debye model. The value for the low-spin isomer was larger than that for the high-spin isomer. The complex $[\text{FeL}^2_2]\text{NCS}$ when freshly recrystallized below 280 K is predominantly in a low-spin state. However, the magnetism at room temperature increases with time, spin-crossover behaviour is exhibited, and the magnetism is dependent on temperature, with a pronounced hysteresis loop of about 70 K at 286 K 10 d after preparation.

Since Cambi and Cagnasso¹ first observed 'magnetic isomerism' for the tris(dithiocarbamato)iron(III) complexes in 1931 there have been numerous reports of spin-crossover iron(II) and iron(III) complexes.²⁻⁶ It is well known that the magnetic behaviours of spin-crossover complexes are variable. Although the hysteresis effect in the temperature dependence of the magnetic behaviour has been observed for many spin-crossover iron(II) complexes,⁷⁻⁹ there has been only one report regarding the hysteresis effect of spin-crossover iron(III) complexes.¹⁰ The two iron(III) compounds examined here are rare examples of compounds with a large hysteresis effect. The chemical structures of the ligands are shown below.



The unique feature of $[\text{FeL}^2_2]\text{NCS}$ is the time and temperature dependences of the magnetism. Such a time dependence was reported for bis[5-methyl-3-(1,10-phenanthroline-2-yl)-1,2,4-oxadiazole]iron(II) tetrafluoroborate.¹¹ It was pointed out that its origin is associated with some slow and minor modification of the crystal lattice.

Spin-crossover complexes showing abrupt transitions at a certain critical temperature T_c often exhibit hysteresis effects and first-order phase transitions.¹² Grinding or ^{60}Co γ -ray irradiation influences the transition behaviour because these operations modify the crystal quality.^{13,14} Therefore, spin-crossover complexes are sensitive to the preparative method and crystallization conditions.¹⁵ In this paper the role of crystal packing is evaluated through a study of the time and temperature dependences of the magnetism.

Experimental

Preparation of the Complexes.— $[\text{FeL}^1_2]\text{ClO}_4$. A mixture of *o*-aminophenol (1.1 g, 10 mmol) in absolute methanol (10 cm³)

and pyridine-2-carbaldehyde (0.7 g, 10 mmol) in absolute methanol (10 cm³) was refluxed for 30 min. Sodium methoxide (0.54 g, 10 mmol) in absolute methanol (25 cm³) was added. Refluxing was continued for 10 min and then the solution was filtered. 2,2-Dimethoxypropane (1 cm³) was added to a solution of $\text{Fe}(\text{ClO}_4)_3 \cdot 6\text{H}_2\text{O}$ (2.2 g, 5 mmol) in methanol (20 cm³) and warmed at 30 °C for 30 min, then slowly added to the above filtrate. The crystals produced were collected by suction and dried in vacuum. Recrystallization from any solvent was not possible since this brought about some decomposition (Found: C, 51.9; H, 3.20; N, 10.1. Calc. for $\text{C}_{24}\text{H}_{18}\text{ClFeN}_4\text{O}_6$: C, 52.45; H, 3.30; N, 10.2%).

The complexes $[\text{FeL}^1_2]\text{X}$ ($\text{X} = \text{NO}_3$, PF_6 , or BPh_4) were also prepared. The hexafluorophosphate complex is in the low-spin state, the nitrate and tetraphenylborate in the high-spin state.

$[\text{FeL}^2_2]\text{NCS}$. This complex was prepared according to the method of Dickinson *et al.*¹⁶ 8-Aminoquinoline (1.44 g, 0.01 mol) and salicylaldehyde (1.22 g, 0.01 mol) were dissolved in methanol (50 cm³), and the mixture was refluxed for 4 h. The cooled solution was mixed with $\text{FeCl}_3 \cdot 6\text{H}_2\text{O}$ (1.35 g, 0.005 mol) in methanol (50 cm³). To this was added, dropwise with stirring, triethylamine (1.10 g, 0.01 mol). The resulting solution was stirred overnight. The chloride complex formed was collected and recrystallized from boiling methanol. The thiocyanate compound was prepared by addition of a hot methanol solution of potassium thiocyanate to a hot methanol solution of the chloride complex. The solid obtained upon cooling was recrystallized from methanol at 280 or 298 K (1 d) (Found: C, 65.0; H, 3.70; N, 11.55. Calc. for $\text{C}_{33}\text{H}_{22}\text{FeN}_5\text{O}_2\text{S}$: C, 65.15; H, 3.60; N, 11.5%).

Physical Measurements.—The magnetic susceptibilities of the polycrystalline samples were measured by the Faraday method using a type 2002 (Cahn Instrument) electrobalance with an electromagnet (8 000 G, 0.8 T). The temperature was controlled over the range 78–320 K by using a digital temperature controller, model 3700 (Scientific Instruments). The magnetic data for one loop were collected in about 7 h. Both heating and cooling rates were controlled manually. The compound $\text{HgCo}(\text{NCS})_4$ was used as a calibration standard. Effective magnetic moments were calculated by use of the formula $\mu_{\text{eff}} =$

† Non-S.I. units employed: B.M. $\approx 9.27 \times 10^{-24}$ A m², a.m.u. = 1.66×10^{-24} g.

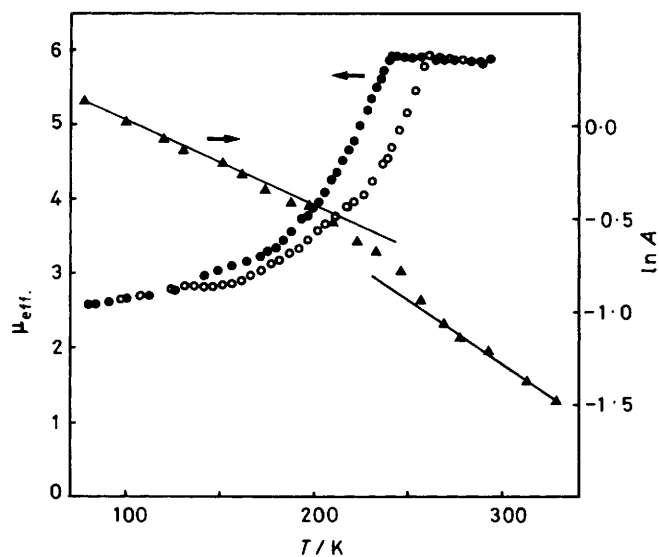


Figure 1. Temperature dependences of the magnetic moment [decreasing temperature (●), increasing temperature (○)] and of $\ln A$ (▲) for $[\text{FeL}^{12}]\text{ClO}_4$.

$2.83 (\chi_M T)^{\frac{1}{2}}$, where χ_M is the molar susceptibility after applying a diamagnetic correction.

Mössbauer spectra were measured with a constant-acceleration spectrometer (Austin Science Associates). Data were stored in a 1 024-channel pulse-height analyzer, type 5200 (Inotech, Inc.). The temperature was monitored with a calibrated copper-constantan thermocouple within a variable-temperature cryostat, type ASAD-4V. A cobalt-57 source of 10 mCi diffused into a palladium foil was used for the absorption measurement. All spectra were fitted by Lorentzian line shapes using a least-squares fitting procedure at the Computer Center, Kyushu University. The velocity scale was normalized with respect to the centre of the spectrum of metallic iron at 296 K. A differential thermal analysis (d.t.a.) measurement was performed in the temperature range 125–373 K with a heating rate of about 2 K min^{-1} using a Shimadzu DT-30 instrument.

Results and Discussion

$[\text{FeL}^{12}]\text{ClO}_4$.—The temperature dependence of the magnetic moment for $[\text{FeL}^{12}]\text{ClO}_4$ was measured in the range 80–293 K, and is illustrated in Figure 1. Fairly abrupt transitions are observed at 242 K in the cooling curve and 262 K in the heating curve, which show phenomenologically the co-operative character. A magnetic hysteresis loop of about 20 K was detected between the heating and cooling temperature curves, but this does not correspond to a normal hysteresis, *i.e.* it is highly asymmetric. The hysteresis width is defined as $\Delta T = T_c - T_c'$, where T_c and T_c' are the critical temperatures (the maximum peak position of the first derivatives of the T curve) for the heating and cooling curves, respectively. It should be noted that the transition at T_c' begins abruptly and the transition at T_c ends abruptly. The slopes of both curves become smooth as the temperature is decreased.

The molar volume of a high-spin isomer $V_M(\text{h.s.})$ is always larger than that of a low-spin isomer $V_M(\text{l.s.})$ and $\Delta V = V_M(\text{h.s.}) - V_M(\text{l.s.})$ is reported¹⁷ to be about $15 \text{ cm}^3 \text{ mol}^{-1}$. It is well known that high-spin isomers produced freshly in low-spin domains by an increase in temperature are believed to be subjected to pressure caused by the surrounding low-spin lattices. If the co-operative effect is strong, production of high-spin isomers will be suppressed and the transition will be higher

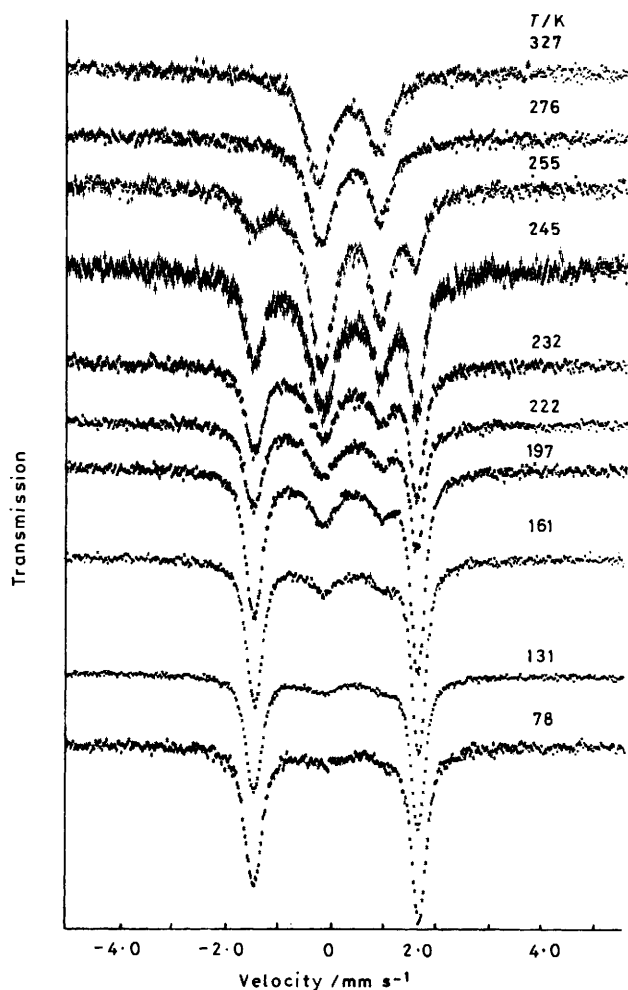


Figure 2. Representative Mössbauer spectra for $[\text{FeL}^{12}]\text{ClO}_4$ at various temperatures (increasing temperature)

than $T_i [= (T_c + T_c')/2]$. Consequently, in the case of a strong co-operative effect and large ΔV , a larger hysteresis loop is expected.^{18,19} It took 7 h to measure the hysteresis loop in this study. If the rate of the transition high spin \rightleftharpoons low spin is low and temperature-dependent, and 7 h is not enough to measure the hysteresis loop under kinetic equilibrium, the observed loop will be asymmetric and a quasi-hysteresis one. Therefore, the slope of the hysteresis curve will become gentle at low temperature.

The temperature dependence of the Mössbauer spectrum of $[\text{FeL}^{12}]\text{ClO}_4$ is shown in Figure 2. The outer doublet of the absorption with quadrupole splitting (q.s.) = 3.176 mm s^{-1} and isomer shift (i.s.) = 0.104 mm s^{-1} at 78 K is assigned to a low-spin isomer in accordance with the magnetic data and its intensity decreases with increasing temperature. The inner doublet, characterized by q.s. = 1.115 mm s^{-1} and i.s. = 0.475 mm s^{-1} at 78 K, gains intensity with increasing temperature, becoming the main peak above 255 K, and is assigned to a high-spin isomer. The temperature dependence of the spectra is characteristic of spin-crossover complexes and is in good agreement with the magnetic data. The Mössbauer parameters at various temperatures are collected in Table 1.

The distortion at an iron nucleus created by the tridentate coordination of five- and six-membered chelate rings of a Schiff base may be larger than that created by individual five- and six-membered chelate rings. The large quadrupole splitting of the low-spin isomer is suggestive of this effect. Furthermore,

Table 1. Mössbauer parameters for $[\text{FeL}^1_2]\text{ClO}_4$ at various temperatures

T K	Low-spin isomer				F(l.s.) %	High-spin isomer				F(h.s.) %	c
	I.s.	Q.s.	Γ_1^a	Γ_h^b		I.s.	Q.s.	Γ_1^a	Γ_h^b		
		mm s ⁻¹									
78	0.104	3.176	0.363	0.314	88.3	0.475	1.115	0.782	0.682	11.7	533
100	0.099	3.160	0.338	0.294	86.7	0.407	1.057	0.793	0.805	13.3	588
120	0.095	3.154	0.342	0.297	86.5	0.406	1.066	0.669	0.447	13.5	577
131	0.089	3.147	0.347	0.302	84.7	0.378	1.077	0.755	0.525	15.3	619
151	0.087	3.142	0.341	0.299	80.6	0.399	1.081	0.749	0.453	19.4	542
161	0.082	3.143	0.349	0.307	78.1	0.387	1.090	0.727	0.520	21.9	508
173	0.079	3.137	0.360	0.304	75.6	0.390	1.108	0.672	0.559	24.4	491
188	0.073	3.130	0.365	0.304	69.6	0.386	1.113	0.676	0.535	30.4	575
197	0.073	3.130	0.365	0.315	70.1	0.379	1.095	0.648	0.533	29.9	521
210	0.069	3.128	0.384	0.310	63.2	0.381	1.091	0.658	0.569	36.8	519
222	0.061	3.126	0.387	0.308	58.6	0.387	1.109	0.665	0.536	41.4	471
232	0.064	3.109	0.392	0.312	50.5	0.374	1.104	0.637	0.588	49.5	499
245	0.053	3.106	0.408	0.338	37.0	0.364	1.113	0.641	0.569	63.0	464
255	0.053	3.107	0.511	0.352	18.8	0.366	1.123	0.604	0.529	81.2	469
268	0.030	3.113	0.466	0.438	6.4	0.357	1.125	0.583	0.501	93.6	497
276						0.358	1.133	0.598	0.535	100.0	524
292						0.345	1.111	0.614	0.598	100.0	478
312						0.328	1.121	0.623	0.542	100.0	468
327						0.319	1.140	0.583	0.577	100.0	468

^a F.w.h.m. for low-energy line. ^b F.w.h.m. for high-energy line. ^c Residual sum for curve fitting.

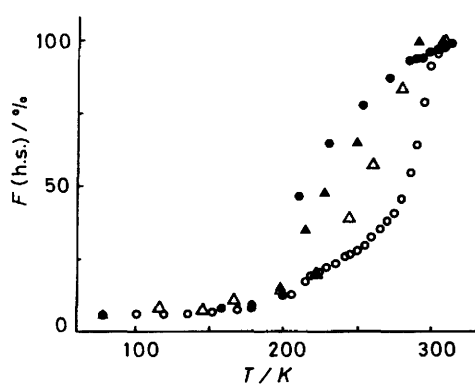


Figure 3. Temperature dependences of the fraction of the high-spin isomer $F(\text{h.s.})$ for $[\text{FeL}^2_2]\text{NCS}$ derived from the magnetic susceptibilities [decreasing temperature (●), increasing temperature (○)] and from the Mössbauer spectra [decreasing temperature (▲), increasing temperature (△)]

the absence of a temperature dependence of the quadrupole splitting in the range 78–268 K suggests that the splitting between the ground and first excited states is large, *i.e.* the anisotropy in bonding is large. The Mössbauer spectra were measured for a tablet of small crystals which were not pulverized, since the magnetic properties are affected by pulverization. The orientation of the crystals, besides the Goldanskii–Karyagin effect and anisotropy of the bonds, must be taken into account when interpreting the spectral asymmetry. However the latter was not pursued further because pulverized samples showed more symmetric spectra at room temperature.

The temperature dependence of the isomer shifts was considerably different for the spin isomers. The effective vibrating mass M_{eff} can frequently be estimated from the second-order Doppler shift, as in equation (1).²⁰ The slopes $d(\text{i.s.})/dT$ for

$$M_{\text{eff}} = -4.168 \times 10^{-2} [d(\text{i.s.})/dT]^{-1} \quad (1)$$

the high- and low-spin isomers are $-(4.74 \pm 0.45) \times 10^{-4}$ and

$-(2.87 \pm 0.39) \times 10^{-4} \text{ mm s}^{-1} \text{ K}^{-1}$ respectively which are smaller than the classical limiting slope of $-7.30 \times 10^{-4} \text{ mm s}^{-1} \text{ K}^{-1}$. The values of M_{eff} estimated for the low- and high-spin isomers are 145 ± 2 and 88 ± 2 a.m. units, respectively. The larger value for the low-spin isomer is understandable because the crystal field of a low-spin isomer is stronger than that for a high-spin isomer, *i.e.* the iron–donor atom bond lengths in low-spin states are 0.13–0.14 Å shorter than in high-spin states.¹⁷

In Figure 1 the values of $\ln A$ are plotted for increasing temperatures, where A is the total absorption area in the Mössbauer spectra. At the spin transition temperature a discontinuous shift from the line corresponding to the low-spin isomer to that for the high-spin isomer is observed because of a difference in the Debye–Waller factors between the isomers. From the slopes of the individual straight lines, Debye temperatures for the two isomers may be estimated. It is clear that the slope for the high-spin isomer is steeper than that for the low-spin isomer. This fact reflects the crystallographic rearrangements accompanying a spin transition and is in accordance with the difference in M_{eff} values. Comparable observations were recently reported for some spin-crossover iron(II) complexes.^{7–9}

$[\text{FeL}^2_2]\text{NCS}$.—The magnetic properties of this complex were initially reported by Dickinson *et al.*¹⁶ However, they did not mention the temperature of preparation. The temperature dependence of the magnetism for $[\text{FeL}^2_2]\text{NCS}$ prepared at 298 K was measured and that for the high-spin isomer fraction is shown in Figure 3 using the correlation $\mu^2 = x\mu_h^2 + (1-x)\mu_l^2$, where the magnetic moment of the high-spin isomer $\mu_h = 5.90$ B.M. and that of the low-spin isomer $\mu_l = 2.03$ B.M. are assumed. Clearly the shape of the cooling curve is different to that of the heating curve and the apparent hysteresis loop was approximately 70 K. The slope of the heating curve is larger than that of the cooling curve. Differences between the slopes of the cooling and heating curves have been observed previously for some iron(II) complexes.^{7–9} There are two transition steps (about 220 and 270 K) in the heating curve, which may suggest the existence of another phase or another isomer with a different transition temperature.

A differential thermal analysis was tried for the samples

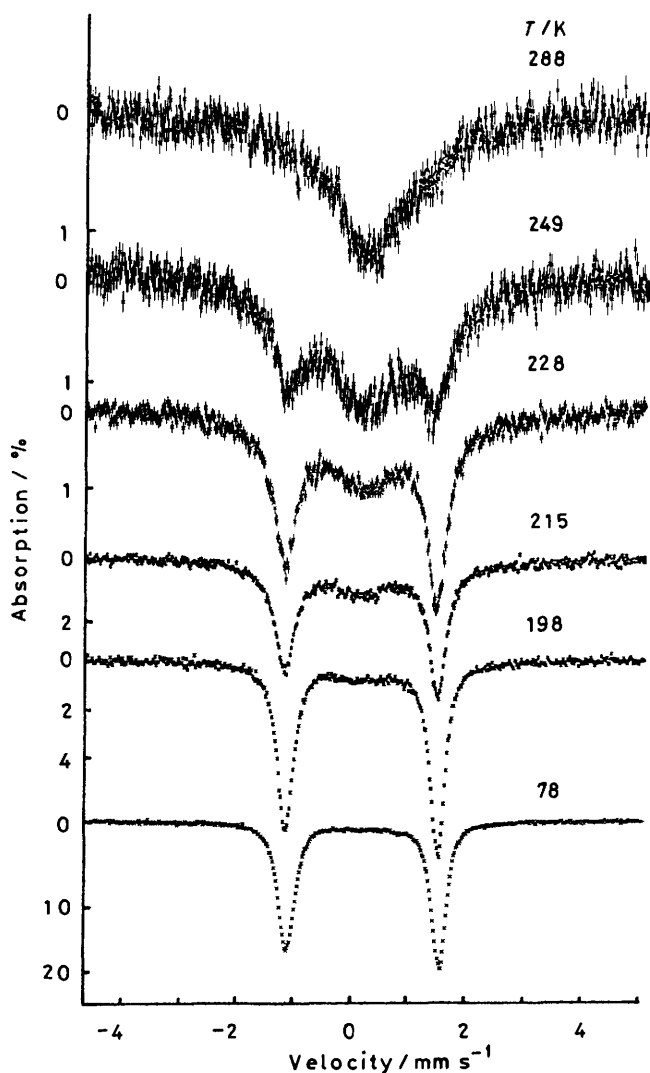


Figure 4. Temperature dependence of the Mössbauer spectra for $[\text{FeL}_2]_2\text{NCS}$ (decreasing temperature)

recrystallized at 298 K, and a weak and broad endothermic peak was observed at 279 K with increasing temperature. However it was too obscure to examine thermodynamic properties. The Mössbauer spectra of $[\text{FeL}_2]_2\text{NCS}$ recrystallized at 298 K were measured at various temperatures and are illustrated in Figures 4 (cooling step) and 5 (heating step), and the parameters are listed in Table 2. The absorption of the high-spin isomer (an inner doublet) is broad and its parameters (i.s. = 0.277 mm s^{-1} and q.s. = 0.467 mm s^{-1} at 223 K in the heating step) are characteristic of high-spin compounds. On the other hand an outer doublet (i.s. = 0.150 mm s^{-1} and q.s. = 2.606 mm s^{-1} at 223 K in the heating step) is characteristic of low-spin compounds and has absorptions of small f.w.h.m. (full width at half maximum).

Population ratios between the high- and low-spin isomers have been estimated from the absorption area in the Mössbauer spectra or from the magnetic susceptibility data. However, the two sets of values are not in agreement as shown in Figure 3. Furthermore, the shapes of the spectra in the cooling step are not in accordance with those in the heating step. As the data in this figure were obtained for samples using the same preparation vessel in order to avoid non-reproducibility, this disagreement may suggest that a gradual spin transition proceeds

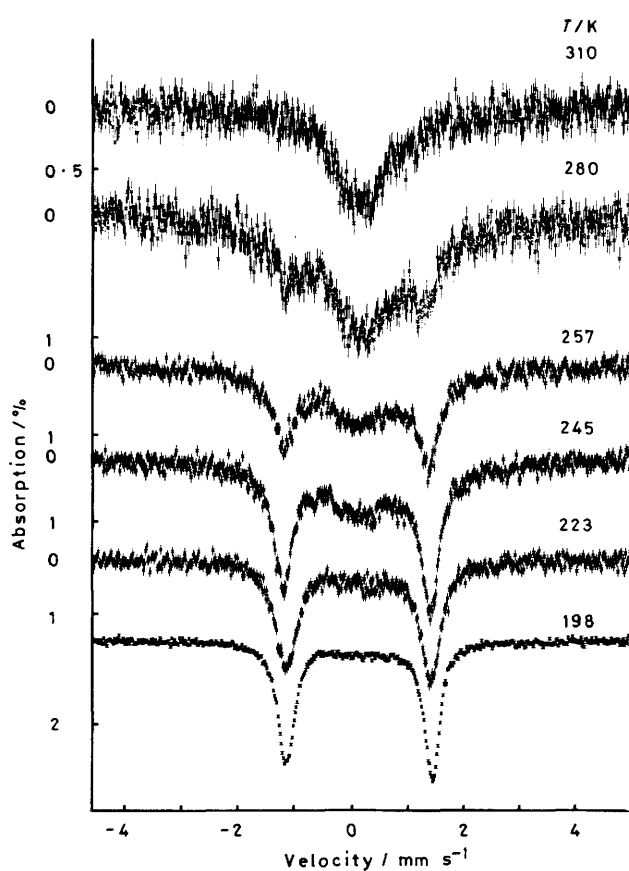


Figure 5. Temperature dependence of the Mössbauer spectra for $[\text{FeL}_2]_2\text{NCS}$ (increasing temperature)

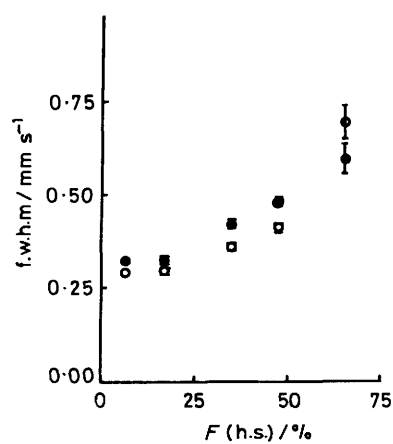


Figure 6. Plots of f.w.h.m. for the high-spin isomer vs. the fraction of high-spin isomer for $[\text{FeL}_2]_2\text{NCS}$ (decreasing temperature). (●) High-energy line; (○) low-energy line

during the measurements. One of the causes for this quasi-hysteresis effect may be the slowness of the transition between the high- and low-spin isomers. However, it is likely that non-equilibrium behaviour of the complexes contributes to the transition process because the second cycle of the magnetic loop resulted in a slightly higher population of the high-spin isomer above 200 K in the heating step than in the first cycle.

It is noticeable that in the cooling step the f.w.h.m. values for the low-spin isomer decrease with decreasing high-spin fraction, as shown in Figure 6. The chemical structure of the low-spin

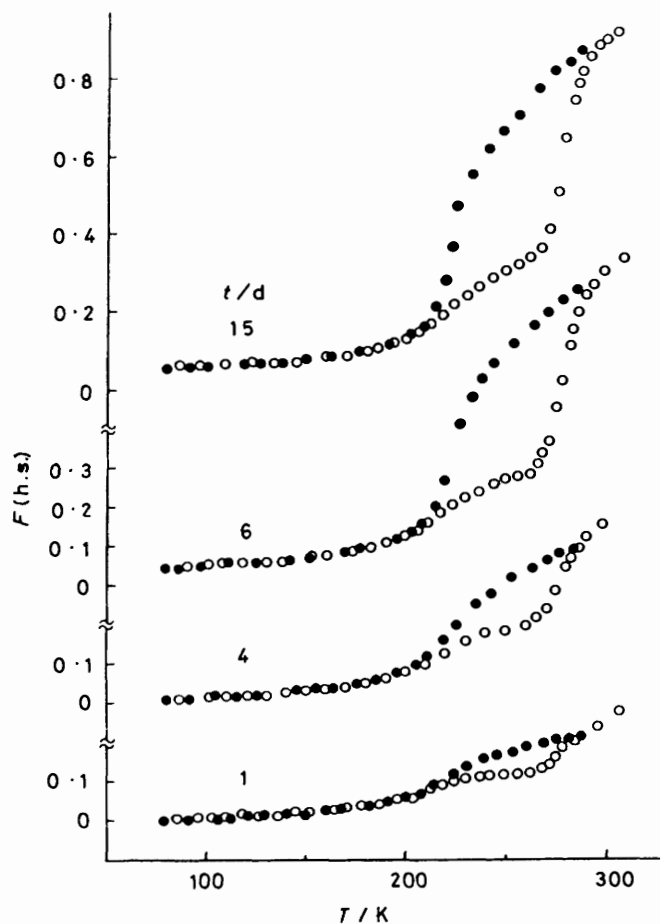


Figure 7. Temperature dependences of the fraction of high-spin isomer for $[\text{FeL}_2]\text{NCS}$ after various periods of agings [decreasing temperature (●), increasing temperature (○)]. The time intervals at 286 K after preparation are shown

isomer which is transformed from the high-spin isomer is initially flexible and becomes rigid with further decrease in temperature. The origin of this temperature dependence may be associated with some slow modification of the crystal lattice and the change in crystal lattice will be simultaneous with the spin transition.

The complex recrystallized below 280 K is predominantly in the low-spin state at room temperature ($\mu_{\text{eff.}} = 2.03$). The unique feature of this complex is the time dependence of the magnetism. The effective magnetic moments at 286 K are 3.26, 4.00, 5.21, and 5.54, 1, 4, 6, and 15 d after preparation, respectively; 1 day after preparation means immediately after filtration of the samples. The temperature dependence of the magnetism of the complex was measured at extended time intervals. The populations of the high-spin isomer determined on the basis of the magnetic data are plotted in Figure 7. The transition behaviour shown in this figure was reproducible if the preparative conditions were exactly the same. Clearly the amount of the 'high-spin' isomer at 286 K increases with time. The transition from low to high spin proceeds to a great extent with aging of the complexes, as is seen from the observation that the magnetic moment becomes 5.54 after aging for 15 d at 286 K. Furthermore, the 'high-spin' complex experiences a transition to the low-spin state at low temperature. Thus, the complex produced by time-aging is a spin-crossover complex. The purity of the sample was confirmed by elemental analyses

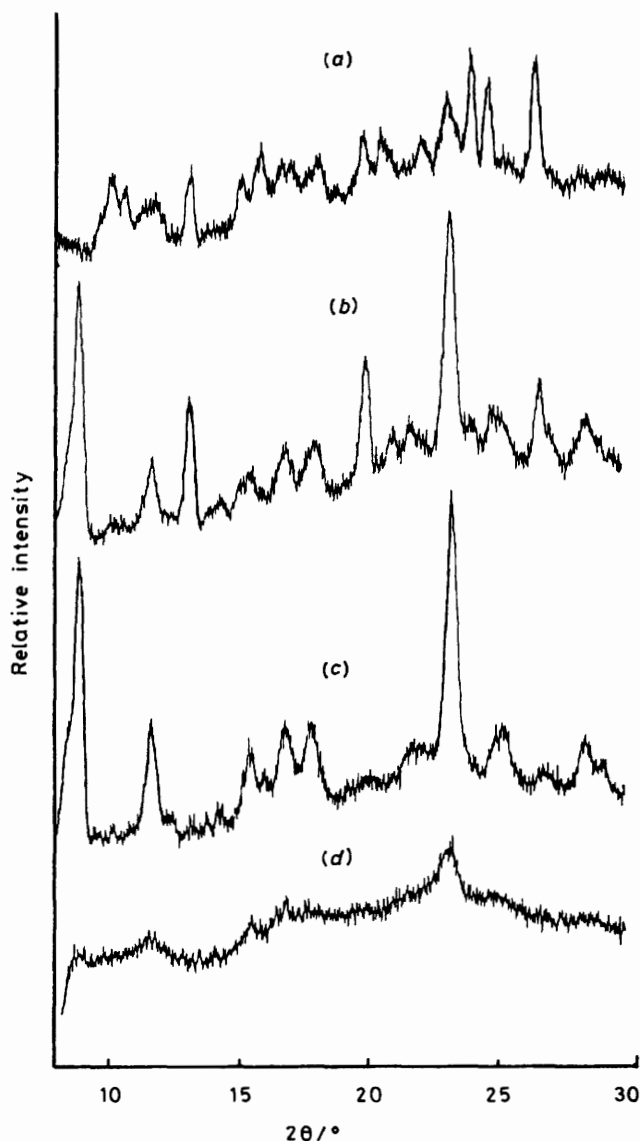


Figure 8. X-Ray powder-diffraction patterns for $[\text{FeL}_2]\text{NCS}$ after various periods of aging and for the ground sample. The samples (a), (b), and (c) were measured after standing at 286 K for 1, 2, and 4 d after preparation (time when the crystals were dissolved in absolute methanol for recrystallization), respectively. Sample (d) was ground using an agate mortar

and i.r. spectroscopy before and after the Mössbauer measurement and the time aging. It should be noted that the transition behaviours (transition temperature range and the width of the apparent hysteresis loops) of samples aged for various times are analogous. This shows that the domain size of the crossover complexes produced in sample (a) in Figure 8 is already larger than a critical size which forms a steady co-operative effect. The general features of the time dependence of the magnetism can be reproduced for samples prepared independently. However, the actual values (width of the hysteresis loop and transition temperature range) may differ slightly from sample to sample. The magnetism of fresh complexes increases rapidly just after the preparation simultaneously with the residual paramagnetic fraction.

X-Ray powder diffraction patterns were measured for the samples immediately after preparation and also at extended

Table 2. Mössbauer parameters for $[\text{FeL}_2]_2\text{NCS}$ at various temperatures

T K	High-spin isomer				Low-spin isomer				c
	Is.	Q.s.	Γ	$F(\text{h.s.})$	Is.	Q.s.	Γ_1^a	Γ_h^b	
	mm s ⁻¹				mm s ⁻¹				
Cooling									
308	0.193	0	1.320	100.0					468
288	0.253	0	1.737	100.0					537
249	0.208	0	1.720	65.3	0.133	2.570	0.694	0.594	442
228	0.219	0	1.758	47.6	0.145	2.651	0.410	0.481	462
215	0.164	0	1.540	35.0	0.148	2.671	0.359	0.420	511
198	0.257	0	1.397	16.6	0.159	2.648	0.296	0.327	584
78	0.360	0	1.075	6.5	0.191	2.660	0.288	0.326	1 227
Heating									
118	0.347 ^d	0.669	0.684	7.4	0.185	2.645	0.298	0.343	625
	0.393	0	1.277	9.1	0.165	2.645	0.298	0.340	659
146	0.391 ^d	0.576	0.528	6.9	0.179	2.642	0.317	0.358	534
	0.401	0	1.057	8.5	0.159	2.643	0.314	0.356	556
167	0.347 ^d	0.598	0.741	10.5	0.164	2.641	0.312	0.354	496
	0.313	0	1.309	13.1	0.145	2.641	0.310	0.350	516
198	0.342 ^d	0.665	0.854	13.4	0.160	2.636	0.318	0.357	547
	0.311	0	1.474	16.7	0.140	2.636	0.316	0.353	568
223	0.277 ^d	0.467	1.018	18.7	0.150	2.606	0.437	0.474	453
	0.294	0	1.320	21.0	0.150	2.606	0.432	0.471	454
245	0.350 ^d	0.686	1.426	38.8	0.134	2.571	0.402	0.447	450
	0.338	0	1.888	42.5	0.133	2.569	0.402	0.441	456
257	0.323	0	1.631	56.9	0.128	2.557	0.447	0.447	495
280	0.290	0	1.711	83.7	0.114	2.454	0.431	0.431	493
310	0.258	0	1.517	100.0					490

^a F.w.h.m. for low-energy line. ^b F.w.h.m. for high-energy line. ^c Residual sum for curve fitting. ^d The spectrum was resolved as a doublet with the same f.w.h.m. values and intensities.

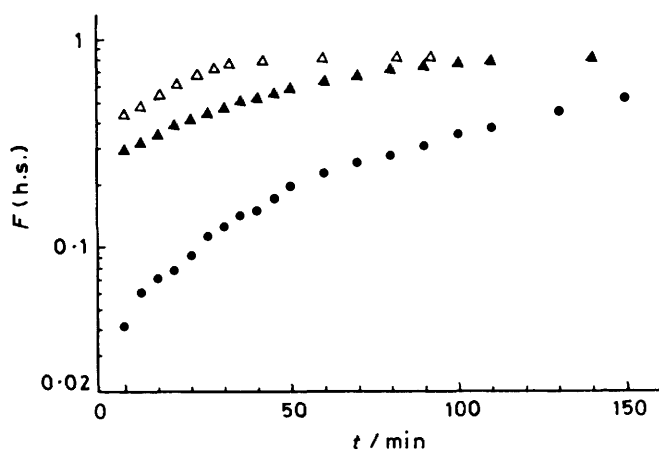


Figure 9. Time dependences of the fraction of the high-spin isomer for $[\text{FeL}_2]_2\text{NCS}$ at various temperatures: 305 (●) K, 310 (▲), and 315 K (△). The data at 286 K are not plotted here because the reaction is too slow

time intervals to examine structural changes. The changes in the patterns are illustrated in Figure 8. The X-ray powder diffraction patterns taken for sample (a) are not superimposable on that for sample (c). Structural changes in a crystal occur slowly with time. Sample (d) pulverized with an agate mortar shows significantly broadened and weak lines, and changes from brown to blue in colour. The domain sizes of the high-spin isomers in sample (a) may be large because the X-ray powder diffraction lines observed are produced by domains of magnitude of about 5 000 Å.

The time dependences of the magnetism of the low-spin complex $[\text{FeL}_2]_2\text{NCS}$ were measured at various temperatures and time dependences of the product (the fraction of the 'high-spin' isomer) determined on the basis of the magnetic data are illustrated in Figure 9. It is clear that the rate of the reaction is dependent on temperature and the transition from a low-spin to a 'high-spin' state is complete in 30 min at 315 K. The large 'high-spin' population at the starting point is due to the experimental limitation; it takes some time to heat the specimens to a certain temperature before measurements are started.

The solid-state reactions can be described empirically by the equation^{21,22} $x = 1 - \exp(-kr^n)$, rearranging to $-\ln[\ln(1-x)] = \ln k + n \ln t$, where x is the fraction reacted after time t and k the reaction rate constant, e.g. $k = 0.55 \text{ min}^{-0.55}$ (at 315 K) was evaluated by plotting $-\ln[\ln(1-x)]$ vs. $\ln t$. Parameter n is a constant that can vary according to the geometry of a system. For this system, $n = 1.2$ (286), 0.82 (305), 0.72 (310), and 0.55 (315 K). The reaction is believed to be complex because n varies widely with temperature, being very sensitive to the progress of the reaction. Also, the hysteresis curve for the sample used for measuring the reaction rate at 315 K was not in perfect agreement with that for the sample used for time-aging at 286 K.

References

- 1 L. Cambi and A. Cagnasso, *Atti Accad. Naz. Lincei, Rend. Cl. Sci. Fis. Mat. Nat.*, 1931, **13**, 809.
- 2 H. Ohshio, Y. Maeda, and Y. Takashima, *Inorg. Chem.*, 1983, **22**, 2684.
- 3 Y. Maeda, N. Tsutsumi, and Y. Takashima, *Inorg. Chem.*, 1984, **23**, 2440.
- 4 N. Matsumoto, K. Kimoto, A. Ohyoshi, and Y. Maeda, *Bull. Chem. Soc. Jpn.*, 1984, **57**, 3307.
- 5 W. D. Federer and D. N. Hendrickson, *Inorg. Chem.*, 1984, **23**, 3861, 3870.

- 6 K. M. Kadish, C. Su, D. Schaeper, C. L. Merrill, and L. J. Wil, *Inorg. Chem.*, 1982, **21**, 3433.
- 7 E. König, G. Ritter, W. Irler, and S. M. Nelson, *Inorg. Chim. Acta*, 1979, **37**, 169.
- 8 E. König, G. Ritter, S. K. Kulshreshtha, J. Waigel, and H. A. Goodwin, *Inorg. Chem.*, 1984, **23**, 1896.
- 9 E. König, R. Ritter, S. K. Kulshreshtha, and S. M. Nelson, *Inorg. Chem.*, 1982, **21**, 3022.
- 10 F. V. Wells, S. W. McCann, H. H. Wickman, S. L. Kessel, D. N. Hendrickson, and R. D. Feltham, *Inorg. Chem.*, 1982, **21**, 2306.
- 11 H. A. Goodwin and F. E. Smith, *Inorg. Nucl. Chem. Lett.*, 1974, **10**, 99.
- 12 M. Sorai and S. Seki, *J. Phys. Soc. Jpn.*, 1972, **33**, 575.
- 13 Y. Maeda, N. Tsutsumi, and Y. Takashima, *J. Radioanal. Nucl. Chem. Lett.*, 1985, **93**, 253.
- 14 E. W. Müller, H. Spiering, and P. Gülich, *Chem. Phys. Lett.*, 1982, **93**, 567.
- 15 P. Ganguli, P. Gülich, E. W. Müller, and W. Irler, *J. Chem. Soc., Dalton Trans.*, 1981, 441.
- 16 R. C. Dickinson, jun., W. A. Baker, and R. L. Collins, *J. Inorg. Nucl. Chem.*, 1977, **39**, 1531.
- 17 E. Sinn, G. Sim, E. V. Dose, M. F. Tweedle, and L. J. Wilson, *J. Am. Chem. Soc.*, 1978, **100**, 3375.
- 18 D. H. Everett and W. I. Whitton, *Trans. Faraday Soc.*, 1952, **48**, 749; D. H. Everett and F. W. Smith, *ibid.*, 1954, **50**, 187; D. H. Everett, *ibid.*, 1954, **50**, 1077; 1955, **51**, 1551.
- 19 A. R. Ubbelohde, *J. Chim. Phys. Phys.-Chim. Biol.*, 1966, **62**, 33.
- 20 R. H. Herber and Y. Maeda, *Inorg. Chem.*, 1980, **19**, 3411.
- 21 B. V. Erofe'ev, *C. R. (Dokl.) Acad. Sci. URSS*, 1946, **52**, 511.
- 22 W. A. Johnson and R. F. Mehl, *Trans. AIME*, 1939, **135**, 416.

Received 13th May 1986; Paper 6/915